so that as time approaches infinity the solution for the radius of the limit cycle, their Equation (62) is

$$r^2 = \frac{1.125 - 0.125\ k_c}{-51.19} \qquad (61)$$

This result indicates that a limit cycle will not be obtained if $k_c < 9$, but will exist if $k_c > 9$, which is exactly the opposite of their conclusions. Since their results do agree with the numerical solutions of the nonlinear equations, it's apparent that including the third derivative term in the approximation changes the topology of the system.

Thermal Instability of a Horizontal Layer of Liquid with Maximum Density

ZU-SHUNG SUN and CHI TIEN

Syracuse University, Syracuse, New York

and YIN-CHAO YEN

U.S. Army Cold Regions Research and Engineering Laboratory, Hanover, New Hampshire

An investigation is carried out to determine the onset of convection of a horizontal layer of liquid subject to temperatures of T_1 and T_2 at lower and upper surfaces, respectively. The liquid is assumed to possess a maximum density value at T_{max} with T_{max} between T_1 and T_2. The temperature-density relationship within the temperature range $|T_1 - T_2|$ can be expressed as $\rho = \rho_{max}\,[1 - \gamma_1 (T - T_{max})^2 - \gamma_2 (T - T_{max})^3]$.

Both rigid-rigid and rigid-free surface conditions were considered. The critical Rayleigh number defined in Equations (20) and (24) is found to be dependent upon two parameters.

Experimental observations on the onset of convection were made and compared with the theoretical results. The experimental work consists of the measurement of the melting rate of a block of ice with melting from both below and above. In all cases, excellent agreement between experimental and theoretical results were obtained.

When a layer of liquid whose density decreases monatomically with the increase of temperature is subject to an adverse temperature gradient, (that is $T_1 > T_2$ where the subscripts 1 and 2 refer to the lower and upper surfaces, respectively) the system is potentially unstable because of its top-heavy situation. The onset of convection is indicated if the Rayleigh number exceeds its critical value. For a liquid with constant thermal expansion coefficient, Rayleigh number is defined as

$$N_{Ra} = \frac{\rho g (T_1 - T_2) d^3}{\nu \kappa} \qquad (1)$$

A somewhat complicated situation arises if the liquid possesses a maximum density over the temperature range $T_2 - T_1$. The liquid density increases upward from the lower surface until it reaches maximum and decreases afterward. Only part of the liquid layer is potentially unstable. Furthermore, the onset of convection is possible with both heating from below and above. For a liquid whose temperature-density relationship can be expressed as

$$\rho - \rho_{max}\,[1 - \gamma\,(T - T_{max})^2] \qquad (2a)$$

and with a definition of Rayleigh number as

$$N_{Ra} = \frac{2\gamma (T_1 - T_{max})\ g (T_1 - T_2) d^3}{\nu \kappa} \qquad (2b)$$

it was found (2, 5, 7) that the critical Rayleigh number which is the criterion for the onset of convection, is dependent upon the temperature difference ratio $(T_1 - T_{max})/(T_1 - T_2)$.

A major limitation of these earlier works is that the particular temperature-density relationship used [that is Equation (2a)] has only a limited range of applicability. For example, in the case of water, the representation of temperature-density data by a parabolic expression is only valid for the temperature of $0 \sim 8$°C. Furthermore, these investigations were restricted to the special case of two rigid boundary surfaces.

The object of the present work is to present a more complete analysis on the effect of liquid maximum density on the thermal instability of a horizontal layer of liquid using a density-temperature relationship with a wider range of applicability. Two types of hydrodynamic boundary conditions, both rigid-rigid and rigid-free surfaces, are considered because of their equal importance. In addition, experimental observations on the onset of convection were also carried out in order to verify the validity of the theoretical results.

ANALYSIS

The pertinent equations of continuity, motion, and energy can be written as:

Zu-shung Sun is at the University of Delaware, Newark, Delaware.

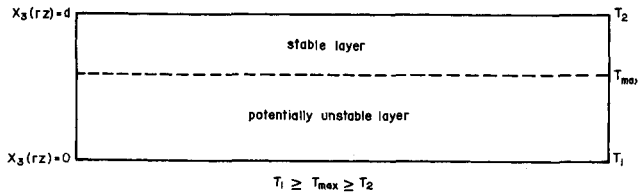

Fig. 1. Illustration of the effect of maximum density on the stability of a horizontal layer heated from below or cooled from the top.

$$\frac{\partial u_i}{\partial x_i} = 0 \tag{3}$$

$$\frac{\partial u_i}{\partial t} + u_j \frac{\partial u_i}{\partial x_j} = -\frac{1}{\rho_0}\frac{\partial P}{\partial x_i} + \left(1 + \frac{\delta\rho}{\rho_0}\right) X_i + \nu \frac{\partial^2 u_i}{\partial x_i \partial x_j} \tag{4}$$

$$\frac{\partial T}{\partial t} + u_j \frac{\partial T}{\partial x_j} = \kappa \frac{\partial^2 T}{\partial x_j \partial x_j} \tag{5}$$

ρ_0 is the density of the fluid at the reference temperature. The coordinates are so taken that x_3 (or z) is opposite to the direction of gravitational force with the fluid layer extending from $z = 0$ to $z = d$. This is shown in Figure 1.

The density temperature relationship within the interested temperature range is assumed to be,

$$\rho - \rho_{max} = -\rho_{max}\left[\gamma_1 (T - T_{max})^2 + \gamma_2 (T - T_{max})^3\right] \tag{6}$$

This expression differs from that of Equation (1) with an additional cubic term. For the case of water, Equation (6) was found to be valid for temperature 0 to 30°C. while Equation (2) is useful only from 0 to 8°C. (6).

The static solutions of velocity and temperature are given as

$$u_i = 0 \tag{7}$$

$$T = T_1 - \beta\lambda_j x_j \tag{8}$$

where λ_j is the unit vector $(0, 0, 1)$, T_1 is the temperature at lower surface, β is the temperature gradient, $(T_1 - T_2)/d$ with T_2 being the temperature at the upper surface.

The density distribution for the static state becomes

$$\rho = \rho_{max}\left[1 - \gamma_1 (T_1 - T_{max} - \beta\lambda_j x_j)^2 - \gamma_2 (T_1 - T_{max} - \beta\lambda_j x_j)^3\right] \tag{9}$$

and the pressure distribution at static state is given as

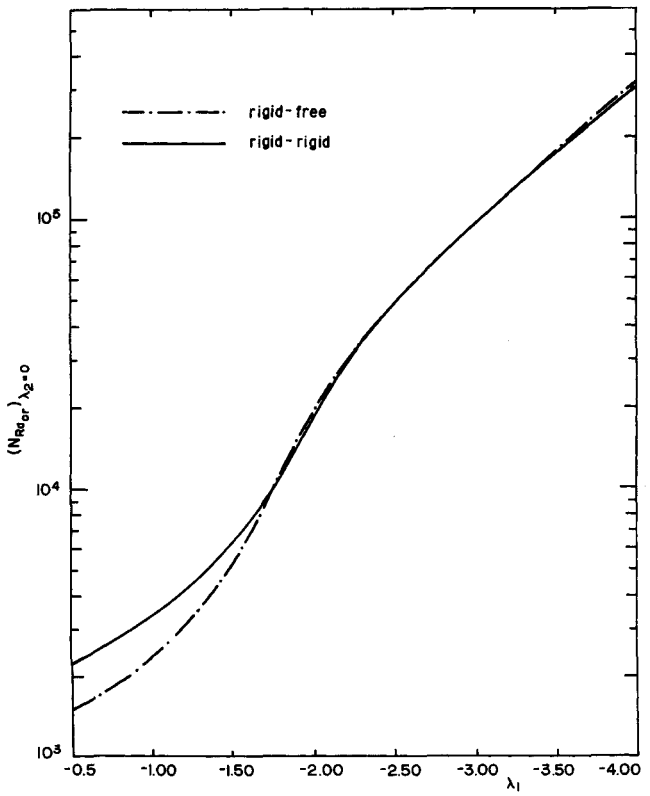

Fig. 2. Critical Rayleigh Number for $\lambda_2 = 0$.

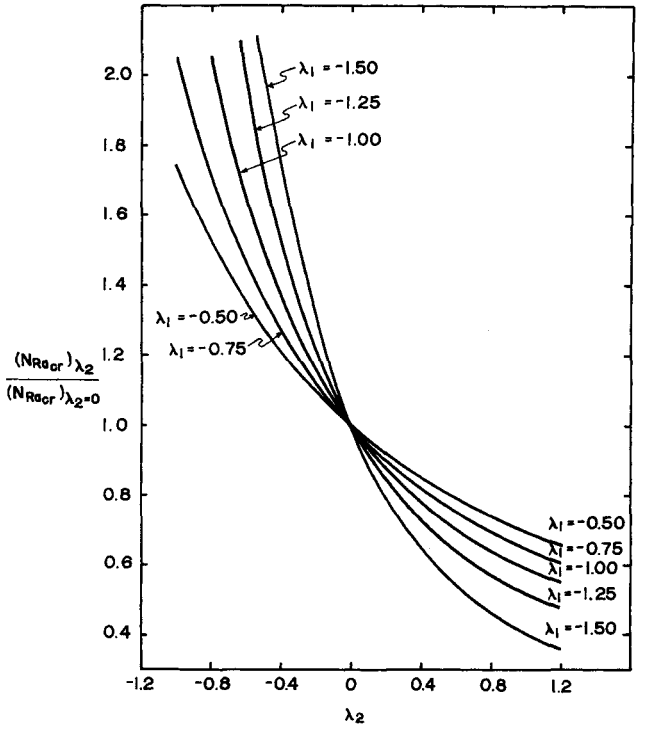

Fig. 3. $\frac{(N_{Ra_{cr}})\,\lambda_2}{(N_{Ra_{cr}})\,\lambda_2 = 0}$ vs. λ_2 with λ_1 as parameter for rigid-free case.

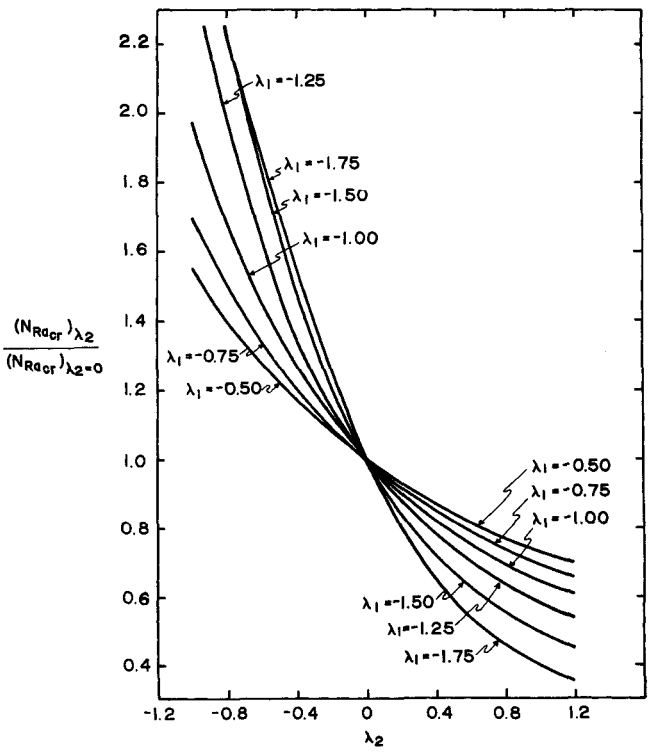

Fig. 4. $\frac{(N_{Ra_{cr}})\,\lambda_2}{(N_{Ra_{cr}})\,\lambda_2 = 0}$ vs. λ_2 with λ_1 as parameter for rigid-rigid case.

TABLE 3. NUMERICAL VALUES OF $(N_{Ra_{cr}})_{\gamma_2=0}$ OBTAINED FROM SUCCESSIVE APPROXIMATIONS

	First Approximation		Second Approximation		Third Approximation		Fourth Approximation		Wave Number	
λ_1	a	b	a	b	a	b	a	b	a	b
−0.5	—	—	—	—	—	—	1,507.83	2,275.32	2.688	3.120
−0.75	—	—	—	—	—	—	1,847.83	2,725.24	2.692	3.121
−1.00	2,366	3,430.15	2,384	3,403.73	2,380.82	3,390.43	2,380.59	3,390.22	2.703	3.126
−1.25	3,294	4,573.53	3,331	4,478.02	3,322.82	4,462.50	3,322.41	4,461.78	2.730	3.143
−1.50	5,417	6,850.29	5,350	6,431.24	5,327.32	6,417.65	5,326.12	6,414.67	2.828	3.190
−1.75	15,134	13,720.58	10,348	10,511.81	10,323.70	10,536.45	10,354.13	10,526.75	3.297	3.404
−2.00	—	—	18,875	18,614.79	—	18,733.44	19,287.52	18,942.44	4.111	4.000
−2.25	—	—	30,543	31,340.00	—	—	32,828.39	32,052.31	4.802	4.685
−2.50	—	—	54,585	53,992.49	—	—	49,280.08	49,741.05	5.372	5.358
−2.75	—	—	132,698	118,687.70	—	—	67,570.13	69,333.44	5.586	5.851
−3.00	—	—	—	—	—	—	95,611.06	95,621.06	6.102	6.076
−3.25	—	—	—	—	—	—	131,286.87	131,217.56	6.655	6.644
−3.50	—	—	—	—	—	—	176,713.69	176,667.12	7.052	7.184
−3.75	—	—	—	—	—	—	236,525.44	236,191.12	7.497	7.595
−4.00	—	—	—	—	—	—	321,294.19	319,671.06	7.912	8.081
−4.25	—	—	—	—	—	—	455,688.56	449,088.19	8.377	8.123

a rigid-free case
b rigid-rigid case

$$\frac{\partial P}{\partial x_i} = -\rho_{\max}\left[1-\gamma_1\left(T_1-T_{\max}-\beta\lambda_j x_j\right)^2 - \gamma_2\left(T_1-T_{\max}-\beta\lambda_j x_j\right)^3\right]\lambda_i g \quad (10)$$

For the perturbed state let u_i determine the velocity, T' and P' the temperature and pressure, respectively.

$$T' = T_1 - \beta\lambda_j x_j + \theta \quad (11)$$

$$P' = P + \delta p \quad (12)$$

The perturbation equations (by dropping second and higher order terms) are found to be

$$\frac{\partial u_j}{\partial x_j} = 0 \quad (13)$$

$$\frac{\partial u_i}{\partial t} = -\frac{1}{\rho_0}\frac{\partial(\delta P)}{\partial x_i} + \nu\nabla^2 u_i + \frac{\rho_{\max}}{\rho_0}\left(T_1-T_{\max} - \beta\lambda_j x_j\right)\cdot\left[2\gamma_1 + 3\gamma_2\left(T_1-T_{\max}-\beta\lambda_j x_j\right)\right] g\theta\lambda_i \quad (14)$$

$$\frac{\partial\theta}{\partial t} = \beta u_j\lambda_j + \kappa\frac{\partial^2\theta}{\partial x_j\partial x_j} \quad (15)$$

Following a procedure commonly employed in linear stability analysis, the details of which can be found elsewhere (4), the problem is reduced to the solution of the following characteristic value equations:

$$(D^2-a^2)\,H = -\left(\frac{\beta}{K}\,d^2\right)W \quad (16)$$

$$(D^2-a^2)^2\,W = \left[\frac{2\gamma_1\,A\Delta T\,gd^2\left(1+\frac{3}{2}\frac{\gamma_2}{\gamma_1}A\Delta T\right)}{\nu}\right](1+\lambda_1 z^+ + a_2 z^{+2})^2\,a^2 H \quad (17)$$

where a is the wave number which characterizes the mode of disturbance, W and H are amplitudes of the disturbances in temperature profile and vertical velocity component, respectively. The operator D, denotes d/dz^+ and

$$z^+ = z/d \quad (18)$$

$$N_{Pr} = \nu/K \quad (19)$$

$$A = \frac{T_1-T_{\max}}{T_1-T_2} \quad (20)$$

$$\lambda_1 = \left(-\frac{1}{A}\right)\left[\frac{1+3\frac{\gamma_2}{\gamma_1}A\Delta T}{1+\frac{3}{2}\frac{\gamma_2}{\gamma_1}A\Delta T}\right] \quad (21)$$

$$\lambda_2 = \frac{1}{A^2}\,\frac{\frac{3}{2}\frac{\gamma_2}{\gamma_1}A\Delta T}{1+\frac{3}{2}\frac{\gamma_2}{\gamma_1}A\Delta T} \quad (22)$$

Equations (16) and (17) can be combined together to yield,

$$(D^2-a^2)^3\,H = -a^2\,N_{Ra}\,(1+\lambda_1 z^+ + \lambda_2 z^{+2})\,H \quad (23)$$

where

$$N_{Ra} = \frac{(2\gamma_1\,A\Delta T)\,g(\Delta T)\,d^3\left(1+\frac{3}{2}\frac{\gamma_2}{\gamma_1}A\Delta T\right)}{\nu\kappa} \quad (24)$$

The boundary conditions are:

$$W = H = 0, \quad z^+ = 0, \text{ and } 1 \quad (25)$$

$$DW = 0, \quad z^+ = 0 \quad (26)$$

and

$$DW = 0 \quad z = 1 \text{ for rigid upper surface} \quad (27a)$$

$$D^2W = 0, \quad z = 1 \text{ for free upper surface} \quad (27b)$$

For the case of rigid-rigid surfaces, the problem becomes identical with that of viscous flow between rotating cylinders as discussed by Steinman (3). The exact counterpart of rigid-free surfaces does not exist in Taylor's problem. Even for the case of rigid-rigid surfaces the results of Steinman (3) cannot be applied to the present problem because of the different ranges of interest of the parameters λ_1 and λ_2 for the respective problem.

The evaluation of the critical Rayleigh number from Equation (23) is carried out according to the general

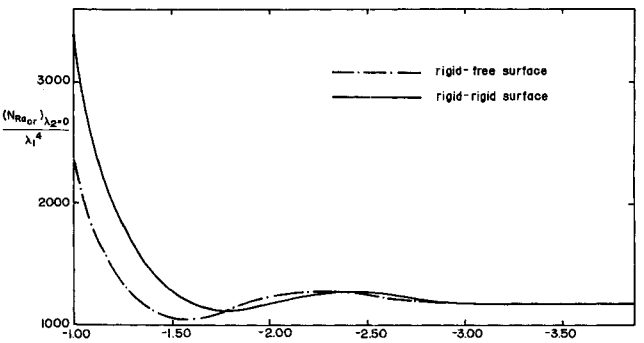

Fig. 5. The asymtotic behavior of $\frac{(N_{Ra_{cr}})\,\lambda_2=0}{\lambda_1^4}$ vs. λ_1.

TABLE 4. COMPARISON OF EXPERIMENTAL AND THEORETICAL RESULTS (MELTING FROM ABOVE)

Run no.	T_2 (°C.)	ν (sq.cm./sec. $\times 10^{-2}$)	α (sq.cm./sec. $\times 10^{-5}$)	d_e (cm.)	λ_1	λ_2	$(N_{Ra})_{cr}$ Experimental	$(N_{Ra})_{cr}$ Theoretical	Sc (cm.)	Deviation in $(N_{Ra})_{cr}$ (%)	Deviation in d (%)
1	6.15	1.602	134	0.68	—1.618	0.112	5,856	6,360	0.699	7.93	2.72
2	10.02	1.512	135	1.16	—2.636	0.298	49,812	48,200	1.147	—3.34	—1.13
3	12.96	1.462	136	1.45	—3.409	0.498	129,189	138,000	1.482	6.39	2.16
4	12.98	1.462	136	1.45	—3.415	0.500	129,388	125,000	1.433	—3.51	—1.19
5	10.05	1.522	135	1.15	—2.644	0.300	48,360	48,200	1.149	—0.33	—0.087
6	7.56	1.582	135	0.85	—1.989	0.170	14,132	15,600	0.878	9.41	3.19
7	13.02	1.462	136	1.40	—3.425	0.503	116,818	125,000	1.432	6.55	2.23
8	7.85	1.582	137	0.85	—2.065	0.183	14,460	15,600	0.872	7.31	2.52
9	7.64	1.582	135	0.85	—2.010	0.173	14,281	15,600	0.875	8.46	2.86
10	13.09	1.441	136	1.38	—3.444	0.508	114,047	125,000	1.423	8.76	3.02
11	6.3	1.622	134	0.72	—1.657	0.118	7,033	6,250	0.692	—12.53	—4.05
12	6.65	1.602	134	0.78	—1.749	0.131	9,556	8,500	0.750	—12.42	—4.00
13	10.25	1.522	135	1.20	—2.696	0.312	56,040	51,000	1.163	— 9.88	—3.18
14	11.75	1.482	135	1.33	—3.091	0.410	89,827	94,000	1.350	4.44	1.48
15	11.92	1.482	135	1.30	—3.136	0.422	85,098	94,000	1.344	9.47	3.27

method developed by Chandrasekhar (*1*). The detailed procedure is given elsewhere (*4*) and will not be repeated here. Briefly speaking, the computation work consists of the finding of the root (Rayleigh number) of an nth order polynomial equation as a function of the wave number, a, for specified parameters λ_1 and λ_2. The minimum value of Rayleigh number is taken as the critical Rayleigh number. A successive approximation method was used in which the order of the polynomial equation was arbitrarily assigned to be a first and increased eventually up to 4.

NUMERICAL RESULTS

The critical Rayleigh number has been computed for both rigid-rigid and rigid-free cases. The ranges of parameters involved are

$$-4.25 < \lambda_1 < -0.5$$
$$-1.4 < \lambda_2 < 1.6$$

The numerical results are summarized in Tables 1 and 2*.

The special case considered earlier corresponds to $\lambda_2 = 0$ since the density-temperature relationship is assumed to be parabolic, that is $\lambda_2 = 0$. For such a case, λ_1 is related only to the temperature differences ratio, A. For the more general case, λ_1 and λ_2 are dependent upon A as well as the temperature coefficients of the density-temperature relationship.

Numerical values of $[(N_{Ra})_{cr}]_{\lambda_2=0}$ evaluated according to different orders of approximation are tabulated in Table 3. For convenience, the results are presented graphically in the form of $(N_{Ra})_{cr}$, vs. λ_1 for $\lambda_2 = 0$. This is shown in Figure 2. The effect of λ_2 on $(N_{Ra})_{cr}$ is indicated through plots of $(N_{Ra_{cr}})_{\lambda_2}/(N_{Ra_{cr}})_{\lambda_2=0}$ vs. λ_2 of various values of λ_1 and is shown in Figures 3 and 4 for rigid-free case and rigid-rigid case, respectively.

As mentioned earlier, in obtaining the critical Rayleigh number, the characteristic equations were solved with successive approximation by assigning arbitrary but increasingly larger values to m and n. However, the complexities of these equations increases rapidly with increasing values of m and n and there is a practical limit to the order of approximation of the numerical computation. Fortunately, for the present work, $(N_{Ra})_{cr}$ converges rapidly with the increase of the order of approximation. For all the cases studied, the maximum order of approximation is 4 (that is $n = m = 4$). A typical example which demonstrates the effect of order of approximation on $(N_{Ra_{cr}})$ is shown in Table 3.

Chandrasekhar (*1*), for the case of rigid-rigid surfaces, gives the asymptotic expression of $(N_{Ra_{cr}})$ for large values of A as

$$(N_{Ra_{cr}}) \sim 1{,}186 \left(\frac{1}{A}\right)^4 \qquad (28)$$

In terms of the present work, this becomes

$$(N_{Ra_{cr}}) \sim 1{,}186\ (\lambda_1)^4 \text{ for } \lambda_2 = 0 \qquad (29)$$

Although this expression is obtained for rigid-rigid surfaces, it should also be applicable to rigid-free case from physical consideration. For a layer of maximum density fluid subject to temperatures from above and below, which are on either side of the maximum density temperature, the density of the fluid first increases upward from the lower surface to a maximum then decreases. The fluid layer, therefore, consists of a potentially unstable layer (with a height of Ad) and a stable layer. The upper boundary effect (that is whether one has free rigid upper surface) is felt only indirectly by the potentially unstable layer. It is obvious that this boundary effect would become less significant as the relative thickness of the stable layer to that of potentially unstable increases, which corresponds to decreasing values of A or increasing value of $-\lambda_1$. For the limiting case of $A \to 0$, $(N_{Ra_{cr}})$ for both cases should become identical.

In order to test this argument, values of $(N_{Ra_{cr}})/\lambda_1^4$ is plotted against λ_1 for $\lambda_2 = 0$. This is shown in Figure 5. Although the curve for the rigid-rigid case differs from that of rigid-free case for small values of $(-\lambda_1)$, both curves approach to the same asymptotic for $(-\lambda_1) > 3.0$ and becomes indistinguishable. The asymptotic expression is found to be

$$(N_{Ra_{cr}})_{\lambda_2=0} \sim 1{,}177\ (\lambda_1)^4 \qquad (30)$$

This is essentially the same as that of Equation (29) with slight difference in coefficient (less than 1%) which, in all probability, can be attributed to errors introduced in the respective numerical computation.

EXPERIMENTAL VERIFICATION

The experimental work reported here was aimed to con-

* Tabular material has been deposited as document 00569 with the ASIS National Auxiliary Publications Service, c/o CCM Information Sciences, Inc, 22 W. 34th St., New York 10001 and may be obtained for $1.00 for microfiche or $3.00 for photocopies.

TABLE 5. COMPARISON OF EXPERIMENTAL AND THEORETICAL RESULTS (MELTING FROM BELOW)

Run no.	T_1 (°C.)	ν (sq.cm./sec. $\times 10^{-2}$)	α (sq.cm./sec. $\times 10^{-5}$)	d_e (cm.)	λ_1	λ_2	$(N_{Ra})_{cr}$ Experimental	$(N_{Ra})_{cr}$ Theoretical	Sc (cm.)	Deviation in $(N_{Ra})_{cr}$ (%)	Deviation in d (%)
1	18.8	1.36	138	0.28	−0.983	−0.311	4,136	4,050	0.278	− 2.12	−0.72
2	18.0	1.36	138	0.30	−1.014	−0.301	4,663	4,021	0.286	−15.97	−4.90
3	7.85	1.58	135	0.93	−1.926	−0.208	16,956	18,400	0.956	7.85	2.72
4	18.8	1.32	138	0.26	−0.983	−0.311	3,412	4,050	0.275	15.75	5.45
5	14.0	1.43	139	0.39	−1.199	−0.255	5,700	5,000	0.373	−14.00	−4.56
6	25.2	1.23	141	0.20	−0.764	0.390	2,826	3,300	0.211	14.36	5.21
7	7.72	1.58	135	1.00	−1.964	−0.208	20,068	21,200	1.019	5.34	1.86
8	10.0	1.52	136	0.56	−1.527	−0.217	7,357	8,200	0.581	10.28	3.61
9	18.83	1.36	138	0.28	−0.982	−0.311	4,149	3,930	0.275	− 5.57	−1.82
10	10.26	1.52	136	0.58	−1.496	−0.218	8,719	7,640	0.555	−14.12	−4.50
11	13.88	1.44	137	0.36	−1.206	−0.254	4,432	5,120	0.378	13.44	4.76
12	17.7	1.36	138	0.27	−1.026	−0.298	3,286	4,020	0.289	18.26	6.57
13	23.2	1.26	139	0.23	−0.830	0.365	3,669	3,500	0.226	− 4.83	−1.77
14	7.7	1.58	135	1.06	−1.970	−0.208	23,718	23,063	1.050	− 2.84	−0.95

firm the theoretical predictions of critical Rayleigh numbers for fluids possessing a density maximum between the lower and upper boundary temperatures T_1 and T_2 and confined between horizontal plates. The experimental apparatus and procedures are described in detail elsewhere (8). Essentially, the apparatus consisted of a lucite cylinder containing homogeneous bubble-free ice conditioned to an initial temperature T_0 before the initiation of the experiment. A copper plate was located at each end of the cylinder acting as either a cold or warm plate. The cold plate was maintained at the initial ice temperature T_0 throughout the experiment. Holes were drilled in the warm plate to allow water to enter the melting chamber to account for the volume shrinkage due to phase change. For each experiment, the warm plate temperature (T_1 for melting from below, T_2 for melting from top) and the amount of water entering into the melting chamber were recorded. From this, the depth of the water layer was computed from the relation $d = V/A(\rho_1 - \rho_2)$ in which V is the volume of water entered up to time t, A is cross-sectional area of the melting chamber, and ρ_1 and ρ_2 are the densities of water and ice, respectively.

A typical curve relating the water layer depth (d) and the time (t) after the initiation of the experiment is shown in Figure 6. For this experiment, T_2 (or the warm plate temperature) was maintained at 10.25°C. The initial ice sample temperature was − 14°C. Also shown in this figure is a curve calculated from Stefan's solution (for this particular pair of temperatures) in which the effect of density inversion and natural convection are not taken into account and conduction is the sole mechanism of heat transfer in the melted water layer. It can be seen that the experimental curve is initially slightly lower than the theoretical curve. The phenomena is reasonable because, in practice, a step temperature rise applied to the boundary cannot be realized. For this particular experiment, it was found that it took 20 min. for the warm plate to reach the desired temperature T_2 (= 10.25°C.). If convective heat transfer were absent in the melted water layer the experimental curve would exhibit the same characteristics of the curve computed from Stefan's solution. Therefore, the transition in the mode of heat transfer in the water layer from conduction to convection can be determined by locating the inflection point (in the d vs. t curve) at which there is a sudden increase in the rate of melting. The water layer depth and time after the initiation of the experiment corresponding to this inflection point are designated as the critical depth, d_e, and critical time, t_c. Altogether 29 experiments were conducted with T_0 ranging from − 6.5 to − 14°C. The effect of T_0 on the value of d_e was found to be insignificant. In 15 of them melting occurred from above. For both cases Equation (24) was used to compute the critical Rayleigh number. For the case when melting occurs from the top, A, as defined in Equation (20), becomes equal to T_{max}/T_2 (T_1 is the melting temperature of ice which is zero degree centigrade), ΔT becomes $(-T_2)$, therefore, Equation (24) reduces to

$$N_{Ra} = \frac{(2\,\gamma_1\,T_{max}\,T_2\,g\,d^3)\left(1-\frac{3}{2}\frac{\gamma_2}{\gamma_1}T_{max}\right)}{\nu\kappa} \tag{24a}$$

On the other hand, for melting from below, T_2 is zero and, therefore, A equals $(1 - T_{max}/T_1)$ and Equation (24) takes the form

$$N_{Ra} = \frac{(2\,\gamma_1\,T_1\,g\,d^3)(T_1-T_{max})\left[1+\frac{3}{2}\frac{\gamma_2}{\gamma_1}(T_1-T_{max})\right]}{\nu\kappa} \tag{24b}$$

By substituting the critical depth d_e determined as described above, for d in Equations (24a) and (24b), values for the experimental critical Rayleigh number were computed and tabulated in Tables 5 and 6 in which values of ν and κ were evaluated at the arithmetic mean of the lower and upper boundary temperatures.

With A and ΔT as defined earlier, Equations (21) and (22) become

$$\lambda_1 = \left(-\frac{T_2}{T_{max}}\right)\frac{\left(1-3\frac{\gamma_2}{\gamma_1}T_{max}\right)}{\left(1-\frac{3}{2}\frac{\gamma_2}{\gamma_1}T_{max}\right)} \tag{21a}$$

and

$$\lambda_2 = -\left(\frac{T_2}{T_{max}}\right)^2\frac{\frac{3}{2}\frac{\gamma_2}{\gamma_1}T_{max}}{\left(1-\frac{3}{2}\frac{\gamma_2}{\gamma_1}T_{max}\right)} \tag{22a}$$

for melting from above, and

$$\lambda_1 = -\left(\frac{T_1}{T_1-T_{max}}\right)\frac{1+3\frac{\gamma_2}{\gamma_1}(T_1-T_{max})}{1+\frac{3}{2}\frac{\gamma_2}{\gamma_1}(T_1-T_{max})} \tag{21b}$$

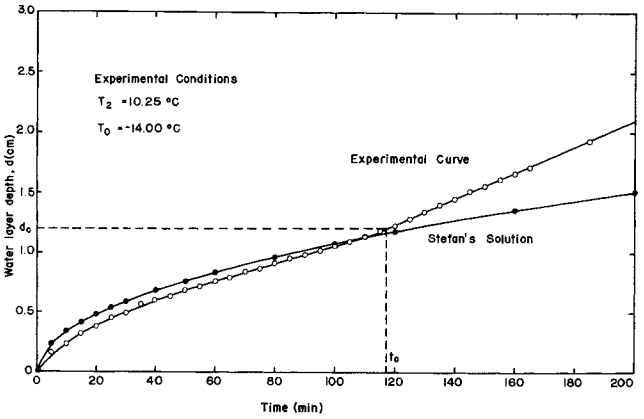

Fig. 6. Experimental detection of the onset of convection.

and

$$\lambda_2 = \left(\frac{T_1 - T_{\max}}{T_1}\right)^2 \frac{\frac{3}{2}\frac{\gamma_2}{\gamma_1}(T_1 - T_{\max})}{1 + \frac{3}{2}\frac{\gamma_2}{\gamma_1}(T_1 - T_{\max})} \tag{22b}$$

for melting from below. With λ_1 and λ_2 computed (see Tables 4 and 5) from Equations (21*a*), (22*a*), (21*b*), and (22*b*), the values for the theoretical $(N_{Ra})_{cr}$ obtained from Table 2 for rigid-rigid surfaces as listed in Tables 5 and 6 were in better agreement with the experimental $(N_{Ra})_{cr}$ than those obtained from Table 1 for rigid-free surfaces.

By letting the theoretical $(N_{Ra})_{cr}$ thus obtained equal to N_{Ra} in Equations (24*a*) and (24*b*), values of d corresponding to these theoretical $(N_{Ra})_{cr}$ were obtained and designated as d_t. These values are also shown in Tables 4 and 5. It should be noticed that the deviation between the values of d_e and d_t is small indeed (maximum deviation 6.57%) while that between the experimental and theoretical $(N_{Ra})_{cr}$ is larger by about a factor of 3 due to the presence of factor d^3 in the definition of the Rayleigh number. A graphical comparison between the experimental and theoretical $(N_{Ra})_{cr}$ for both cases of melting is shown in Figure 7. Within the experimental error, it can be concluded that the experimental values of $(N_{Ra})_{cr}$ are in complete agreement with those predicted by the analytical results presented in this paper.

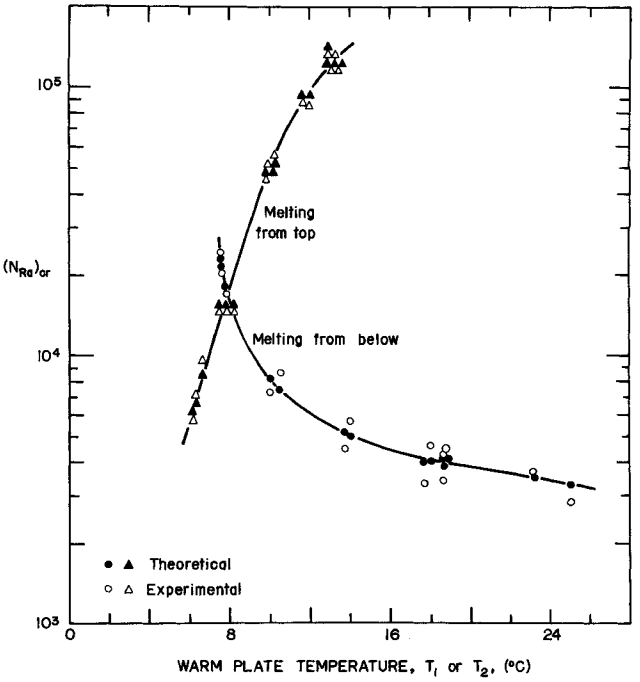

Fig. 7. Comparison of theoretical and experimental results.

ACKNOWLEDGMENT

Part of this work was performed under Grant No. DA-AMC-27-021-65-G16 and DA-AMC-27-021-G20, US. Army Cold Regions Research and Engineering Laboratory, Hanover, New Hampshire and carried out at Syracuse University. The authors also wish to thank Syracuse University Computing Center for the use of its facilities.

NOTATION

a = dimensionless wave number
A = temperature difference ratio, defined by Equation (25)
d = height of liquid layer, cm.
D = operator, defined as d/dz^+
g = gravitational acceleration, cm./sec.^{2}
H = quantity associated with temperature disturbance
N_{Pr} = Prandtl number, defined by Equation (19)
N_{Ra} = Rayleigh number, defined by Equations (1), (2*b*) or (24)
$N_{Ra_{cr}}$ = critical Rayleigh number
p = pressure, dyne/sq.cm.
P' = pressure at perturbed state, dyne/sq.cm.
T = temperature, °C.
T' = temperature at perturbed state, °C.
$T_{\max}$ = maximum density temperature, °C.
T_1, T_2 = lower and upper surface temperature, respectively, °C.
u_i = velocity vector, cm./sec.
W = quantity associated with velocity disturbance
x_i = coordination, cm.
z^+ = dimensionless vertical distance defined as z/d

Greek Symbols

β = temperature gradient defined as $(T_1 - T_2)/d$, °C./cm.
$\delta\rho$ = density difference, g./cc.
ρ = density, g./cc.
$\rho_{\max}$ = maximum density, g./cc.
ρ_0 = reference density, g./cc.
κ = thermal diffusivity, sq.cm./sec.
λ_1, λ_2 = parameters defined by Equations (21) and (22), respectively
λ_j = unit vector, (0, 0, 1)
γ_1, γ_2 = temperature coefficients of density-temperature relationship, see Equation (9), $(°C.)^{-2}$, $(°C.)^{-3}$, respectively
θ = temperature difference defined by Equation (11), °C.
ν = kinematic viscosity, sq.cm./sec.

LITERATURE CITED

1. Chandrasekhar, S., "Hydrodynamic and Hydromagnetic Stability," Claventon Press, Oxford (1961).
2. Debler, W. R., *J. Fluid Mech.*, **24**, 165 (1966).
3. Steinman, H., *Quart. Appl. Math.*, **14**, 27 (1956).
4. Sun, Zu-Shung, MS thesis, Syracuse Univ., New York (1968).
5. Tien, C., *AIChE J.*, **14**, 652 (1968).
6. Vanier, C. R., and C. Tien, *Chem. Eng. Sci.*, **22**, 1747 (1968).
7. Vernois, G., *Astrophysical J.*, **137**, 647 (1963).
8. Yen, Y. C., C. Tien, and Gary Sanders, *Proc. Third Intern. Heat Transfer Conf.*, **4**, 159 (1966).

Manuscript received April 11, 1968; revision received June 28, 1968; paper accepted July 1, 1968.